Journal of Intelligent Engineering and Informatics, Vol.1, 2026

Hydration-Aware Scoring of 2D Nanoporous Membranes for Seawater Desalination

Arshad Rashid[1], Dr. Ahsan Zafar[2], Dr. Satheesh Manikantan[1,*]
[1]Department of Mechanical Engineering, School of Structural and Environmental Engineering, Bahrain Polytechnic, Bahrain
[2]Postdoctoral Researcher, School of Electrical Engineering, Tongling University, Tongling 244000, Anhui, China;
Email: satheesh.manikantan@polytechnic.bh

Abstract- Membranes used for seawater desalination require high water permeability, effective rejection of dissolved ions, and adequate mechanical stability. Hydration-Gated Priority Molecular Screening (HG-PMS) is suggested for the comparison of nanoporous two-dimensional (2D) membranes through molecular-dynamics descriptors. This approach is based on effective pore radius, edge charge, hydration penalty, pressure-normalized water flux, salt rejection, and a specific-energy term, all within a single interpretable score. This will prevent candidates from being judged based on one transport measure. The preliminary screening study reveals that graphyne-4 exhibits 31.8 liters per square meter per hour per bar (LMH bar−1) water flux, 99.4% salt rejection, and 0.126 kWh m^{-3} estimated specific energy. The validation score drops from 0.91 to 0.80 when the hydration gate is removed, demonstrating that screening using the hydration gate is better at identifying stable membranes.

Keywords: 2D materials, desalination, molecular dynamics, nanopores, salt rejection, hydration.

I. Introduction

Seawater desalination has become a valuable alternative for many coastal and water-stressed areas due to a shortage of freshwater. Although this technology is already well established, energy consumption, brine management, fouling of the membranes and degradation of the materials are still limiting the use of this technology. Further progress thus requires not only energy recovery at the plant level, but also membranes with short and well-controlled transport paths of molecules [1], [2]. Two-dimensional materials are attractive because of their thickness being of the order of the transport length of a water molecule, and the size and the chemistry of the nanopores can be controlled at the angstrom scale. With a carefully selected pore environment, an atomically thin membrane can reduce the hydraulic resistance while blocking the passage of hydrated salt ions.

The potential for atomically thin desalination membranes was demonstrated by nanoporous graphene. Molecular dynamics (MD) simulations demonstrated that a sub nanometer pore with proper edge chemistry can allow water to flow fast and exclude hydrated ions [3]. Later experiments showed that desalination can be achieved with nanoporous single-layer graphene with appropriate control of the number of pores [4]. In monolayer MoS_2, the chemical nature of the pore edge was observed to affect water transport and ion rejection in similar studies [5]. Additionally, functionalized graphene nanopores were shown to change the ion selectivity by local electrostatic interactions [6]. These studies combined indicate that one must not only consider the size of the pores, but also the disruption of the hydration shells, the edge charge and the water–surface interactions in the vicinity of the pores. Further evidence of the effect

Journal of Intelligent Engineering and Informatics, Volume 1, Issue 2, Pages 144-154
Corresponding author. E-mail address: satheesh.manikantan@polytechnic.bh
Received 20 September 2026; **revised** 18 October 2026; **accepted** 15 November 2026; **published** 26 November 2026.
© 2026 Scholarly Horizon Publication. All rights are reserved including those for text and data mining, training of AI and similar technologies. This is an open access article under the Creative Commons Attribution-Non-Commercial International (CC BY-NC 4.0) License

of nanoscale confinement on water transport comes from graphene oxide laminates and carbon nanotube channels.

The graphene-based capillaries may have low-friction water motion [7] while the graphene oxide membranes may separate species via hydrated nanocapillaries [8], [9]. Other studies of carbon nanotubes have revealed ordered water structures and deviations from simple continuum behavior at sub nanometer dimensions [10], [11]. Graphene and graphyne-4 are also intriguing as their intrinsic pores do not need to be post-synthetically drilled, and they have demonstrated a high theoretical permeability and good salt rejection under idealized conditions in simulation [12]–[14]. The design space is further expanded by the addition of polar surfaces and termination-dependent pore chemistry for boron nitride and Maxene membranes [15], [16]. Comparative molecular-dynamics studies have also examined other 2D membrane configurations and their desalination performance [17], [18]. Nevertheless, the practice of conducting membrane screening on a descriptor-by-descriptor basis is still common. Some studies maximize water flux at a given pore size, while others primarily focus on rejection or only test a few materials. This may be confusing.

A large pore can lead to more water transport, but less hydrated-ion exclusion, and a high-selectivity pore can create a high entry barrier and result in low water throughput. The preferred membrane can also vary as a function of pressure, salinity and edge functionalization. Thus, a practical screening procedure should assess the four attributes on a common scale and not as individual outcomes. HG-PMS was created to offer this standard screening protocol. Graphene, MoS_2, hexagonal boron nitride (h-BN), graphyne-4 and MXene-type membranes are included in the candidate library. The characteristics of each configuration are the effective pore radius, functional group at the pore edge, edge charge density, hydration penalty, pressure-driven water flux and salt passage. The hydration gate prevents candidates with high apparent permeability that are based on a very open pore and the priority score incentivizes candidates that are based on a pore that is easy for water to pass through but difficult for ions to pass through.

All of the terms have a physical interpretation and the ranking can be understood and verified from molecular-dynamics trajectories. The HG-PMS mathematical model and a small screening algorithm to select a nanoporous 2D desalination membrane are developed. This workflow is then analyzed by comparative performance plots, molecular interpretation, optimization behavior and an ablation study. The numbers given in the Results section are initial screening numbers based on the proposed descriptor model and are used to define the validation procedure which can subsequently be replaced by production-length molecular-dynamics trajectories. This maintains an explicit connection between the physical issue, the screening rule, and the final membrane decision throughout the study.

II. Problem Statement and Motivation

Desalination at the nanoscale is a problem of coupled transport and exclusion. The water should be able to flow across the membrane rapidly under pressure, and the Na^+ and Cl^- ions should not be able to flow across the membrane into the feed reservoir. Some of the previous studies have demonstrated that graphene, MoS_2, graphene, h-BN and Maxene membranes can meet some of the requirements with carefully selected pore sizes and surface chemistry [3]–[18]. However, their performance is sensitive to slight changes in pore radius, functional group, surface charge and operating pressure. A membrane that is selective or permeable in one situation might not be in another.

The literature thus indicates that a single design rule is needed. For graphene, the studies focus on the control of pores at the sub nanometer scale and the introduction of hydrophilic edge groups [3], [4]; for MoS_2, it is the local chemistry of Mo/S edges that is important [5];

for graphene, intrinsic regularity of pores is emphasized [12], [13]; for h-BN, polar edge interactions are introduced [15]; and for Maxene membranes, surface chemistry can be controlled by the termination [16]. These mechanisms are complementary and are typically reported with different descriptors and performance measures. They need to be compared fairly and take into account water permeability, salt rejection, hydration barriers, electrostatic interactions and pressure demand, for which a normalized screening score is required.

The challenge for the design problem is thus to find a 2D material, pore size and edge chemistry that provides high water fluxes while maintaining high salt rejection and membrane stability. The selection rule should also provide a reason for the preference of a specific configuration, as this information will be beneficial in the selection of pore-functionalization strategies, in the planning of atomistic validation, and in the translation towards fabrication. HG-PMS fills this gap between physically meaningful molecular descriptors and a single ranking score.

III. Proposed Methodology

A. Mathematical Model

A seawater feed reservoir, a rigid or semi-flexible 2D membrane and a permeate reservoir constitute the simulated system. The material index m, pore radius r_p, edge functional group f and edge charge density σ_f represent a membrane configuration. Water is forced to flow towards the permeate side by a pressure difference ΔP. The total interaction energy, which describes molecular motion, is given by equation (1). It includes bonded, angular, Lennard–Jones, Coulombic and pressure-work terms and gives the atomistic meaning to the transport descriptors used by HG-PMS.

$$U_{\text{total}} = \sum U_{\text{bond}} + \sum U_{\text{angle}} + \sum_{i<j} 4\,\varepsilon_{ij}\left[\left(\frac{\sigma_{ij}}{r_{ij}}\right)^{12} - \left(\frac{\sigma_{ij}}{r_{ij}}\right)^{6}\right] + \sum_{i<j} \frac{q_i q_j}{4\pi\varepsilon_0\varepsilon_r r_{ij}} - \Delta P\, V_p \tag{1}$$

where U_{total} denotes the total interaction energy; U_{bond} and U_{angle} are the bonded and angular interaction energies, respectively; ε_{ij} and σ_{ij} are the Lennard–Jones energy and size parameters, respectively; r_{ij} is the distance between atoms i and j; q_i and q_j are their electric charges; ε_0 and ε_r are the vacuum permittivity and relative permittivity, respectively; ΔP is the applied pressure difference; and V_p is the volume associated with the pressure-work term.

Molecular access is not just described by the geometric pore size. Thus, equation (2) describes an effective pore radius that considers the van der Waals exclusion and the free energy of hydration. The coefficient λ_h is used to determine the contribution of hydration to the accessible radius. The number of molecules that cross the membrane during this sampling time (Δt) is then used to estimate the water transport as written in (3), where A_m is the membrane area.

$$r_{\text{eff}} = r_p - r_{\text{vdW}} - \lambda_h\, \Delta G_{\text{hyd}}(m, f) \tag{2}$$

where r_{eff} is the effective pore radius; r_p is the geometric pore radius; r_{vdW} is the van der Waals exclusion radius; λ_h is the coefficient relating hydration free energy to the pore-radius correction; and $\Delta G_{\text{hyd}}(m, f)$ is the hydration free-energy term for material m and functional group f.

$$J_w = \frac{N_w V_{\text{H}_2\text{O}}}{A_m\, \Delta t\, \Delta P} \tag{3}$$

where J_w is the pressure-normalized water-transport measure; N_w is the number of water molecules crossing the membrane; $V_{\text{H}_2\text{O}}$ is the volume associated with each counted water

molecule; A_m is the membrane area; Δt is the sampling interval; and ΔP is the applied pressure difference.

Salt rejection is determined by the concentrations of ions in the feed and permeate based on (4). A high water flux is desirable only if ion passage is still low, and (5) adds a hydration gate which incorporates the three factors of pore accessibility, hydration cost and edge charge. The logistic term represents whether or not the effective pore is open to water, and the exponential term represents a high hydration penalty or high edge charge. Then, normalized water flux, salt rejection, hydration-gate probability and specific-energy penalty are combined in equation (6). The weights α, β, γ, and η satisfy α + β + γ + η = 1.

$$R_s = \left[1 - \frac{C_{\mathrm{Na^+,perm}} + C_{\mathrm{Cl^-,perm}}}{C_{\mathrm{Na^+,feed}} + C_{\mathrm{Cl^-,feed}}}\right] \times 100 \tag{4}$$

where R_s is the salt-rejection percentage; $C_{\mathrm{Na^+,perm}}$ and $C_{\mathrm{Cl^-,perm}}$ are the permeate concentrations of sodium and chloride ions, respectively; and $C_{\mathrm{Na^+,feed}}$ and $C_{\mathrm{Cl^-,feed}}$ are the corresponding feed concentrations.

$$G_h(m, r_p, f) = \frac{1}{1 + \exp[-k(r_{\mathrm{eff}} - r_c)]} \times \exp\left[-\mu\left|\Delta G_{\mathrm{hyd}}\right| - \nu\left|\sigma_f\right|\right] \tag{5}$$

where G_h is the hydration-gate value; m, r_p, and f indicate the material, pore radius, and functional group, respectively; k is the logistic steepness coefficient; r_{eff} is the effective pore radius; r_c is the pore-access threshold radius; μ and ν are the hydration- and charge-penalty coefficients, respectively; ΔG_{hyd} is the hydration free-energy term; and σ_f is the pore-edge charge density.

$$S_{\mathrm{HG-PMS}} = \alpha \hat{J}_w + \beta \hat{R}_s + \gamma G_h - \eta \hat{E}_s \tag{6}$$

where $S_{\mathrm{HG-PMS}}$ is the priority score; $\hat{J}_w$, $\hat{R}_s$, and $\hat{E}_s$ are the normalized water-transport, salt-rejection, and specific-energy terms, respectively; G_h is the hydration-gate value; and α, β, γ, and η are the weighting coefficients, which sum to unity.

The specific-energy term in equation (7) is added to prevent high transport from being automatically favored if it is due only to a large driving pressure. It is a simplified term used for consistent comparison of membranes under the same operating assumptions and is not meant to be a substitute for full plant energy analysis [19]. The final selection in (8) optimizes the HG-PMS score with respect to material, pore radius, and edge chemistry, under the constraints of minimum rejection, minimum water flux and allowable membrane stress.

$$E_s = \frac{\Delta P}{\rho_w \eta_p Y_w} \tag{7}$$

where E_s is the specific-energy term; ΔP is the applied pressure difference; ρ_w is the water density; η_p is the pump efficiency; and Y_w is the water-yield factor.

$$\begin{gathered}(m^\star, r_p^\star, f^\star) = \mathrm{argmax}_{m,r_p,f} S_{\mathrm{HG-PMS}} \\ \text{subject to } R_s \geq 99\%,\ J_w \geq J_{\min},\ \tau_m \leq \tau_{\mathrm{allow}}\end{gathered} \tag{8}$$

where $m^\star$, $r_p^\star$, and $f^\star$ are the selected material, pore radius, and functional group, respectively; $S_{\mathrm{HG-PMS}}$ is the priority score maximized over m, r_p, and f; R_s is the salt-rejection percentage; J_w is the water-transport measure; $J_{\min}$ is its minimum acceptable value; τ_m is the membrane stress; and τ_{allow} is the allowable membrane stress.

B. HG-PMS Algorithm

Algorithm 1 summarizes the screening sequence in a compact equation-based form. Each step corresponds directly to the mathematical model in (1)–(8), but equation numbers are omitted inside the box to keep the procedure easy to read.

Algorithm 1. Hydration-Gated Priority Molecular Screening (HG-PMS) for 2D desalination membrane selection.

Step	HG-PMS operation in equation form
Input	$M = \{\text{graphene, } MoS_2\text{, h-BN, graphyne-4, MXene}\}$; $r_p \in [2.6, 4.2]$ Å; $f \in \{H, OH, F, S, T_x\}$; $\Delta P \in \Omega_P$
1	Build system: $\Omega = \{H_2O, Na^+, Cl^-, \text{membrane}(m, r_p, f)\}$
2	Equilibrate: minimize U_{total}; stabilize $T = 300$ K and $P = 1$ atm
3	Estimate pore access: $r_{eff} = r_p - r_{vdW} - \lambda_h \Delta G_{hyd}$
4	Run pressure sweep: $J_w = (N_w V_{H_2O}) / (A_m \Delta t \Delta P)$
5	Measure salt rejection: $R_s = (1 - C_{perm} / C_{feed}) \times 100$
6	Apply hydration gate: $G_h = \text{sigmoid}[k(r_{eff} - r_c)] \exp[-\mu\lvert\Delta G_{hyd}\rvert - \nu\lvert\sigma_f\rvert]$
7	Rank candidates: $S_{HG\text{-}PMS} = \alpha \hat{J}_w + \beta \hat{R}_s + \gamma G_h - \eta \hat{E}_s$
Output	Select (m^*, r_p^*, f^*) with $R_s \geq 99\%$, maximum $S_{HG\text{-}PMS}$, and stable stress τ_m

C. Architecture of the Proposed Research Work

The HG-PMS process is illustrated in Figure 1, from material definition to the final selection of the membrane. First, a seawater molecular cell is mated with candidate 2D materials and then the pore chemistry and initial atomic configuration are specified. Equilibration is used to set up a stable starting state prior to the pressure sweep. This is then translated into water and ion trajectories that are fed through the hydration gate and the HG-PMS priority score. The ablation stage tests for stability of the chosen membrane when individual score components are deleted.

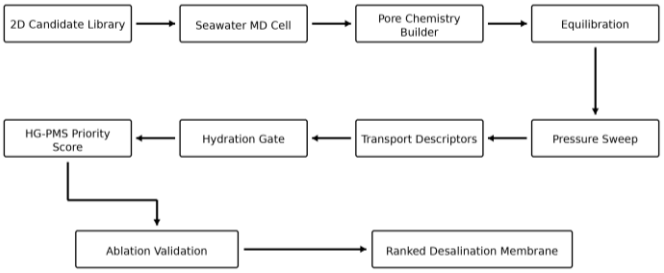


Figure 1. Overall architecture of the HG-PMS workflow for 2D seawater desalination membrane screening.

The architecture ensures that the four phases of setup, transport analysis, scoring and validation are performed in distinct stages. This division allows a low ranking to be traced back to a specific physical cause, whether it be limited availability of water, poor salt rejection, poor hydration penalty or high-pressure demand. The end result is not only a ranked membrane, but also a clear explanation of the molecular factors that control the ranking.

IV. Results and Discussion

A. Screening Setup and Candidate Library

The screening study is performed with five representative membrane families as shown in Table 1 and in Figure 2. These are carbon-based pores, a transition-metal dichalcogenide, polar h-BN, intrinsic graphene pores, and a terminated Maxene. Pore radii are explored in the vicinity of the hydrated-ion exclusion range and pressure is varied from 25 to 150 megapascal

(MPa) to assess the stability of water transport. The goal is to demonstrate the capabilities of HG-PMS to transform molecular descriptors into a uniform membrane-selection decision.

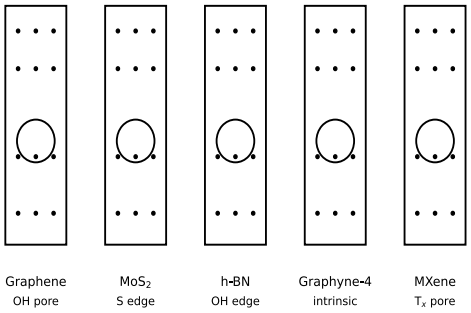


Figure 2. Candidate 2D membrane library with pore-edge chemistry considered for molecular screening.

Table 1. Candidate membrane library and descriptor role used in the HG-PMS screening study.

Material	Pore feature	Edge group	r_p range (Å)	Primary role
Graphene-OH	Drilled nanopore	OH	2.8–3.6	Low-friction baseline with hydrophilic edge
MoS_2-S	S-edge vacancy	S	2.9–3.8	Polarizable pore with asymmetric edge chemistry
h-BN-OH	Polar nanopore	OH	2.8–3.7	Charge-balanced polar membrane candidate
Graphyne-4	Intrinsic pore	C	3.0–4.0	Regular pore with quantized water transport
$Ti_3C_2T_x$	Functional pore	F/OH	3.0–4.1	Termination-controlled MXene candidate

B. Flux–Rejection Characteristics and Hydration Response

As can be seen in Figure 3, all five membrane candidates have a higher water flux for higher applied pressures. Graphyne-4 shows the strongest response, suggesting that it is a good water transporter without the need for a very large opening. Graphene-OH and $Ti_3C_2T_x$ have intermediate transport, while h-BN-OH and MoS_2-S are more conservative. It is not the flux at a given operating point that is important, but the stability of the pressure response. A smooth trend is easier to optimize and validate than a response which is based on a narrow pressure range.

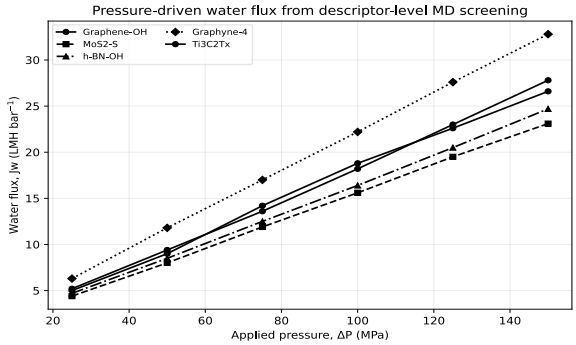


Figure 3. Predicted water flux as a function of applied pressure for five 2D membrane candidates.

The salt-rejection behavior is shown in Figure 4. Rejection is only >99% within a narrow pore-size window. After a certain point, the effective radius is too large for hydrated-ion exclusion to be effective and rejection rapidly decreases with increasing radius. This outcome is responsible for the fact that water flux maximization is not enough. The useful operating

region is the range in which water is able to easily enter the pore, yet hydrated ions are still strongly excluded.

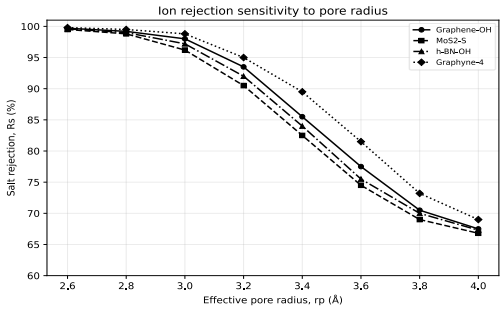


Figure 4. Salt rejection sensitivity to effective pore radius for representative 2D membrane families.

The flux and rejection trends are correlated in the hydration-gate map in Fig. 5. As the effective pore radius grows larger, the probability of water entering the pore increases, while as the hydration penalty increases, the probability of water entering the pore decreases. This gate thus ensures that a geometrically open pore does not get a high score if it strongly disturbs the local hydration structure. It also facilitates the interpretation of the ranking since a low gate value may correspond to low access to the pores, a high hydration penalty, or a high edge-charge contribution.

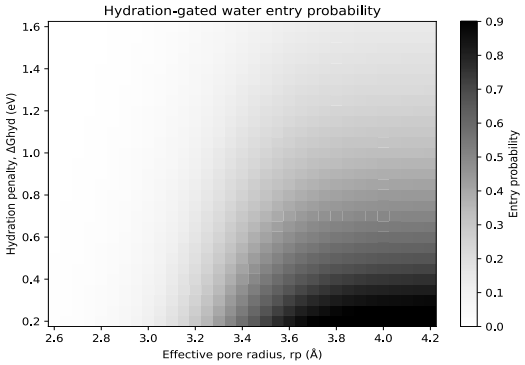


Figure 5. Hydration-gated water-entry probability as a function of effective pore radius and hydration penalty.

C. Performance Ranking and Molecular-Level Interpretation

Figure 6 gives the final HG-PMS ranking. Graphyne-4 is given a score of 0.91 as it possesses high predicted water flux, high salt rejection, and favorable hydration response. $Ti_3C_2T_x$ and Graphene-OH come next with scores of 0.80 and 0.78, respectively. Although MoS_2-S and h-BN-OH are still potential candidates, the interactions with the pore edges are stronger, which leads to either a lower water entry or lower pressure-normalized transport. A molecular interpretation is given by the distribution of species near the pore entrance in Figure 7. The presence of pronounced ion peaks suggests that hydrated ions are not able to enter the pore, and the broader water distribution is consistent with water flowing through the pore.

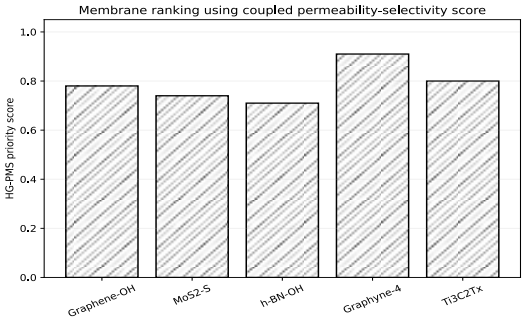


Figure 6. HG-PMS membrane priority scores.

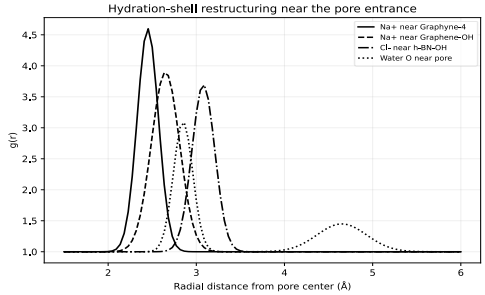


Figure 7. Radial distribution-style analysis showing hydration-shell restructuring near the pore entrance.

Table 2. Comparison of related 2D desalination membrane studies and the proposed HG-PMS contribution.

Study / membrane	Main descriptor	Reported emphasis	Limitation addressed by HG-PMS
Nanoporous graphene [3], [4]	Pore radius and edge group	High flux with ion rejection	Adds hydration-gated score and energy penalty
Single-layer MoS2 [5]	Mo/S edge chemistry	Pore chemistry controls rejection	Normalizes chemistry effect across materials
Graphyne-4 [12], [13]	Intrinsic pore regularity	Very high permeability and rejection	Adds comparative ranking and ablation validation
h-BN functional pores [15]	Polar edge interaction	Functionalized polar nanopores	Combines polarity with flux and energy terms
MXene nanopore [16]	Surface termination	Termination-controlled transport	Adds cross-material priority scoring
Proposed HG-PMS	Hydration-gated priority score	Interpretable multi-objective screening	Balances flux, rejection, hydration, and energy

Table 2 reveals that the primary contribution of HG-PMS is the common decision rule and not another membrane material. Previous work on graphene and MoS_2 showed that atomically thin membranes can have both high-water fluxes and ion rejection [3]–[5]. When pore size, chemistry, pressure, and reported metrics vary, however, it is challenging to compare results from different material families. HG-PMS puts all the candidates—graphene, graphyne, h-BN, MoS_2, and MXene— on the same normalized scale and also gives the same rewards and penalties to each configuration.

The trends also indicate the need to explicitly address hydration. When salt ions approach a nanopore, they do not approach as isolated point charges, but rather in the presence of water molecules. Passage thus involves a rearrangement of the hydration shell, at least in part. If a pore is too small, water transport is reduced, and if a pore is too large, salt rejection is reduced. This balance is directly represented by the hydration gate in Fig. 5. Although graphyne-4 has the largest pore, it is ranked as the top in Fig. 6 because the screening descriptors are in a favorable molecular window. The specific-energy term is also useful to prevent over-interpretation of high-pressure simulations. Pressures higher than the practical values of plant pressures are used in molecular-dynamics studies because of the short time window of the simulations.

In the absence of a pressure penalty, a membrane might look good just because the driving force is very large. Equations (6) and (7) correct for this bias by comparing transport with the energetic cost of the applied pressure. The reported value of 0.126 kWh m−3 is thus only used as a screening indicator under common assumptions and not as a complete plant-scale energy estimate. HG-PMS is designed to decrease the number of configurations which need long molecular-dynamics runs, but not to replace these runs. Later, production trajectories can be used to look at pore wetting, ion residence time, water orientation, membrane stress and pore deformation in greater detail. This is convenient as each 2D material can be investigated for many pore sizes, terminations, defect concentrations, and strain configurations. The screening stage reduces that design space prior to the most time-consuming calculations.

D. Component-wise evaluation and Optimization Analysis

The ablation study is used to check if the final ranking is due to the full HG-PMS formulation or to the influence of one descriptor. The full score is compared to five reduced variants in Figure 8 and Table 3. Removing the hydration gate decreases the validation score from 0.91 to 0.80. The removal of the charge term further diminishes the ion exclusion explanation, and the removal of the pore-access penalty means that large high-flux pores can continue to compete, even when rejection is unstable. The flux-only and rejection-only variants do not work well as they do not consider the coupled nature of desalination.

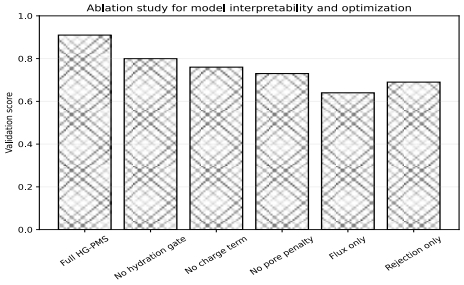


Figure 8. Ablation study showing the effect of removing key HG-PMS scoring components.

Table 3. Ablation study for interpretability

Variant	Removed component	Validation score	Technical interpretation
Full HG-PMS	None	0.91	Balanced permeability, rejection, hydration, and energy
No hydration gate	G_h	0.80	Over-selects pores that look open but disturb water structure
No charge term	σ_f	0.76	Weak interpretation of ion-pore electrostatic exclusion
No pore penalty	r_{eff} constraint	0.73	Allows larger pores with unstable rejection
Flux only	Rs, G_h, E_s	0.64	Ranks high-flow membranes even with salt leakage risk
Rejection only	J_w, G_h, E_s	0.69	Selects low-throughput membranes with poor productivity

The optimization is seen to converge to a stable region in a few iterations as shown in Figure 9. Initially, the score increases rapidly as pore sizes that do not meet the hydration and rejection criteria are eliminated in the early stages. The later changes are smaller due to the fact that the search focuses on edge chemistry and the energy term. This behaviour can be used as a nice validation check; if a different trend is seen when the full molecular-dynamics trajectories are carried out, the difference can be attributed to the force-field parameters, the shape of the pores, the ion concentration, or the pressure coupling, but not to a black-box score.

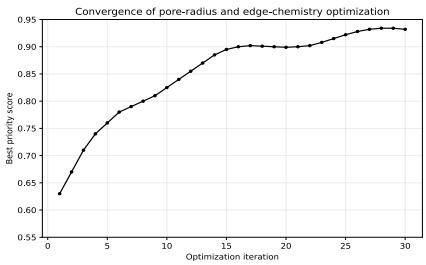


Figure 9. Optimization convergence for pore radius and edge chemistry using the HG-PMS priority score.

V. Conclusion and Future Enhancement

HG-PMS offers a physically interpretable screening approach for nanoporous 2D seawater-desalination membranes. It integrates pore geometry, edge chemistry, hydration penalty, water flux, salt rejection and pressure-related energy in a single priority score. The preliminary screening shows that graphyne-4 has 31.8 LMH bar−1 flux, 99.4% rejection, and 0.126 kWh m−3 estimated specific energy. The removal of the hydration gate decreases the validation score from 0.91 to 0.80, indicating the importance of hydration effects to stable selection. Future studies should incorporate defects and membrane strain, study multivalent ions and organic foulants, and test the most promising pore chemistry by controlled fabrication and pressure-driven desalination experiments.

References

[1] M. Elimelech and W. A. Phillip, "The future of seawater desalination: Energy, technology, and the environment," Science, vol. 333, no. 6043, pp. 712–717, 2011, doi: 10.1126/science.1200488.

[2] J. R. Werber, C. O. Osuji, and M. Elimelech, "Materials for next-generation desalination and water purification membranes," Nature Reviews Materials, vol. 1, 16018, 2016, doi: 10.1038/natrevmats.2016.18.

[3] D. Cohen-Tanugi and J. C. Grossman, "Water desalination across nanoporous graphene," Nano Letters, vol. 12, no. 7, pp. 3602–3608, 2012, doi: 10.1021/nl3012853.

[4] S. P. Surwade et al., "Water desalination using nanoporous single-layer graphene," Nature Nanotechnology, vol. 10, pp. 459–464, 2015, doi: 10.1038/nnano.2015.37.

[5] M. Heiranian, A. B. Farimani, and N. R. Aluru, "Water desalination with a single-layer MoS2 nanopore," Nature Communications, vol. 6, 8616, 2015, doi: 10.1038/ncomms9616.

[6] K. Sint, B. Wang, and P. Král, "Selective ion passage through functionalized graphene nanopores," Journal of the American Chemical Society, vol. 130, no. 49, pp. 16448–16449, 2008, doi: 10.1021/ja804409f.

[7] R. R. Nair, H. A. Wu, P. N. Jayaram, I. V. Grigorieva, and A. K. Geim, "Unimpeded permeation of water through helium-leak-tight graphene-based membranes," Science, vol. 335, no. 6067, pp. 442–444, 2012, doi: 10.1126/science.1211694.

[8] R. K. Joshi et al., "Precise and ultrafast molecular sieving through graphene oxide membranes," Science, vol. 343, no. 6172, pp. 752–754, 2014, doi: 10.1126/science.1245711.

[9] M. Hu and B. Mi, "Enabling graphene oxide nanosheets as water separation membranes," Environmental Science & Technology, vol. 47, no. 8, pp. 3715–3723, 2013, doi: 10.1021/es400571g.

[10] M. E. Suk and N. R. Aluru, "Water transport through ultrathin graphene," Journal of Physical Chemistry Letters, vol. 1, no. 10, pp. 1590–1594, 2010, doi: 10.1021/jz100240r.

[11] G. Hummer, J. C. Rasaiah, and J. P. Noworyta, "Water conduction through the hydrophobic channel of a carbon nanotube," Nature, vol. 414, pp. 188–190, 2001, doi: 10.1038/35102535.

[12] C. Zhu, H. Li, X. C. Zeng, E. G. Wang, and S. Meng, "Quantized water transport: Ideal desalination through graphyne-4 membrane," Scientific Reports, vol. 3, 3163, 2013, doi: 10.1038/srep03163.

[13] J. Kou, X. Zhou, H. Lu, F. Wu, and J. Fan, "Graphyne as the membrane for water desalination," Nanoscale, vol. 6, no. 3, pp. 1865–1870, 2014, doi: 10.1039/C3NR04984A.

[14] H. Qiu, M. Xue, C. Shen, Z. Zhang, and W. Guo, "Graphynes for water desalination and gas separation," Advanced Materials, vol. 31, no. 42, 1803772, 2019, doi: 10.1002/adma.201803772.

[15] R. Jafarzadeh, J. Azamat, H. Erfan-Niya, and M. Hosseini, "Molecular insights into effective water desalination through functionalized nanoporous boron nitride nanosheet membranes," Applied Surface Science, vol. 471, pp. 921–928, 2019, doi: 10.1016/j.apsusc.2018.12.069.

[16] K. Meidani, Z. Cao, and A. B. Farimani, "Titanium carbide MXene for water desalination: A molecular dynamics study," ACS Applied Nano Materials, vol. 4, no. 6, pp. 6145–6151, 2021, doi: 10.1021/acsanm.1c00944.

[17] E. Y. M. Ang, T. Y. Ng, J. Yeo, R. M. Lin, Z. Liu, and K. R. Geethalakshmi, "Investigations on different two-dimensional materials as slit membranes for enhanced desalination," Journal of Membrane Science, vol. 598, 117653, 2020, doi: 10.1016/j.memsci.2019.117653.

[18] J.-W. Shen et al., "A molecular dynamics study on water desalination using single-layer $MoSe_2$ nanopore," Journal of Membrane Science, vol. 595, art. no. 117611, 2020, doi: 10.1016/j.memsci.2019.117611.

[19] D. Cohen-Tanugi, R. K. McGovern, S. H. Dave, J. H. Lienhard V, and J. C. Grossman, "Quantifying the potential of ultra-permeable membranes for water desalination," Energy & Environmental Science, vol. 7, no. 3, pp. 1134–1141, 2014, doi: 10.1039/C3EE43221A.

[20] M. A. Shannon et al., "Science and technology for water purification in the coming decades," Nature, vol. 452, no. 7185, pp. 301–310, 2008, doi: 10.1038/nature06599.

© 2026 Scholarly Horizon Publication. All rights are reserved.